

# Anaerobic oxidation of methane coupled to nitrate reduction in a novel archaeal lineage

Mohamed F. Haroon<sup>1\*</sup>, Shihu Hu<sup>2\*</sup>, Ying Shi<sup>2</sup>, Michael Imelfort<sup>1,2</sup>, Jurg Keller<sup>2</sup>, Philip Hugenholtz<sup>1,3</sup>, Zhiguo Yuan<sup>2</sup> & Gene W. Tyson<sup>1,2</sup>

Anaerobic oxidation of methane (AOM) is critical for controlling the flux of methane from anoxic environments. AOM coupled to iron<sup>1</sup>, manganese<sup>1</sup> and sulphate<sup>2</sup> reduction have been demonstrated in consortia containing anaerobic methanotrophic (ANME) archaea. More recently it has been shown that the bacterium *Candidatus 'Methyloirabilis oxyfera'* can couple AOM to nitrite reduction through an intra-aerobic methane oxidation pathway<sup>3</sup>. Bioreactors capable of AOM coupled to denitrification have resulted in the enrichment of '*M. oxyfera*' and a novel ANME lineage, ANME-2d<sup>4,5</sup>. However, as '*M. oxyfera*' can independently couple AOM to denitrification, the role of ANME-2d in the process is unresolved. Here, a bioreactor fed with nitrate, ammonium and methane was dominated by a single ANME-2d population performing nitrate-driven AOM. Metagenomic, single-cell genomic and metatranscriptomic analyses combined with bioreactor performance and <sup>13</sup>C- and <sup>15</sup>N-labelling experiments show that ANME-2d is capable of independent AOM through reverse methanogenesis using nitrate as the terminal electron acceptor. Comparative analyses reveal that the genes for nitrate reduction were transferred laterally from a bacterial donor, suggesting selection for this novel process within ANME-2d. Nitrite produced by ANME-2d is reduced to dinitrogen gas through a syntrophic relationship with an anaerobic ammonium-oxidizing bacterium, effectively outcompeting '*M. oxyfera*' in the system. We propose the name *Candidatus 'Methanoperedens nitroreducens'* for the ANME-2d population and the family *Candidatus 'Methanoperedenaceae'* for the ANME-2d lineage. We predict that '*M. nitroreducens*' and other members of the '*Methanoperedenaceae*' have an important role in linking the global carbon and nitrogen cycles in anoxic environments.

*Methanoperedenaceae* fam. nov.

*Candidatus 'Methanoperedens nitroreducens'* gen. et sp. nov.

**Etymology.** *Methanoperedens*. *methano* (new Latin): pertaining to methane; *peredens* (Latin): consuming, devouring; *nitroreducens*. *nitro* (new Latin): pertaining to nitrate; *reducens* (Latin): leading back, bringing back and in chemistry converting to a different oxidation state. The name implies an organism capable of consuming methane and also reducing nitrogen-related compounds.

**Locality.** Enriched from a mixture of freshwater sediment and anaerobic wastewater sludge in Brisbane, Australia.

**Diagnosis.** Anaerobic, methane-oxidising, nitrate-reducing archaeon belonging to the *Methanoperedenaceae* fam. nov. (-aceae ending to denote a family). Grows as irregular cocci 1–3 µm in diameter and is typically found as sarcina-like clusters. Growth occurs at mesophilic temperatures (22–35 °C)<sup>5</sup>, pH 7–8 (refs 4, 5).

Microorganisms are central to the global methane cycle. Approximately 300 teragrams (Tg) of methane are produced annually through methanogenesis<sup>6</sup>, of which 90% is consumed by specialized groups of

archaea, collectively called ANME, that anaerobically oxidize methane before it diffuses into oxic environments<sup>7</sup>. AOM is proposed to occur by reversal of the canonical methanogenesis pathway based on incomplete metabolic reconstructions from three partial ANME-1 genomes<sup>8–10</sup>, protein immunodetection<sup>11</sup> and *in vitro* enzymatic assays<sup>12</sup>. However, validation of reverse methanogenesis in ANME remains to be demonstrated and has been hampered by an inability to obtain a pure culture.

AOM has been studied mostly in ANME-1 and ANME-2 that work in concert with sulphate-reducing bacteria (SRB); a process by which methane is oxidized to carbon dioxide and sulphate is reduced to hydrogen sulphide<sup>6</sup>. Recently, it has been suggested that ANME can couple AOM to sulphate reduction directly<sup>13</sup>. AOM can also be coupled to denitrification, as shown by the discovery of nitrite-driven aerobic methane oxidation in '*M. oxyfera*'<sup>3</sup>. ANME-2d has previously been co-enriched with '*M. oxyfera*' in bioreactors fed with methane and nitrate, raising the possibility that this ANME group may be involved in AOM coupled to nitrate reduction<sup>14</sup>. Given the prevalence of nitrate in the environment, verification of nitrate-driven AOM (as opposed to sulphate or nitrite as terminal electron acceptors) may have important implications for global methane cycling.

Here, an anaerobic laboratory-scale bioreactor was pulse-fed with nitrate, ammonium and methane for 350 days (see rationale below). Process data indicated simultaneous AOM, nitrate reduction and anammox (Fig. 1a). Fluorescence *in situ* hybridization (FISH) and 16S rRNA gene amplicon profiling revealed that the bioreactor community was dominated by ANME-2d (78% relative abundance; Fig. 1b, Supplementary Table 1 and Supplementary Fig. 1) making it a likely candidate responsible for the observed AOM. Notably, '*M. oxyfera*' and known SRB were not detected in the bioreactor community (Supplementary Table 1), eliminating the possibility that these populations contribute to nitrite- or sulphate-driven AOM, respectively. Organisms related (99% sequence identity) to the anammox bacterium, *Candidatus 'Kuenenia stuttgartiensis'*<sup>15</sup>, were present as a flanking population (approximately 3% relative abundance).

To confirm the predicted role of ANME-2d, we performed metagenomic sequencing of the bioreactor community. We assembled 13.3 gigabase pairs (Gb) of 150-bp paired-end Illumina HiSeq2000 data into 18,805 contigs (Supplementary Table 2) and separated the ANME-2d population from the flanking community based on guanine–cytosine content, read coverage and tetranucleotide frequencies (Supplementary Table 3 and Supplementary Figs 2–4). High relative abundance and a distinctive archaeal genome signature expedited this process. Six other genomes including the *Kuenenia* population could be resolved similarly (Supplementary Fig. 4). The ANME-2d contigs were reduced to 10 scaffolds using 3-kb-insert mate-pair sequence data (Supplementary Figs 5 and 6). Single-copy gene analysis confirmed completeness and fidelity of the genome (Supplementary Table 4). The genome size and guanine–cytosine content are 3.2 megabase pairs

<sup>1</sup>Australian Centre for Ecogenomics, School of Chemistry and Molecular Biosciences, The University of Queensland, Brisbane, Queensland 4072, Australia. <sup>2</sup>Advanced Water Management Centre, Faculty of Engineering, Architecture and Information Technology, The University of Queensland, Brisbane, Queensland 4072, Australia. <sup>3</sup>Institute for Molecular Bioscience, The University of Queensland, Brisbane, Queensland 4072, Australia.

\*These authors contributed equally to this work.

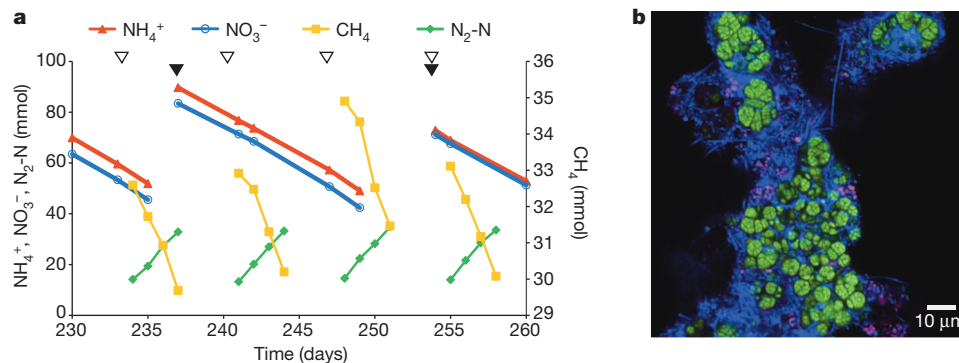


**Figure 1 | Bioreactor performance data and microbial community composition.** **a**, Key bioreactor performance data during steady-state operation from day 230 to 260 after inoculation. The arrows indicate pulse-feeding events of nitrate and ammonium (black), and methane (white). Nitrate, ammonium and methane consumption, and dinitrogen gas production, can be

(Mb) and 43%, respectively, comparable to a previously sequenced ANME-1b genome<sup>9</sup> (Supplementary Table 5 and Supplementary Fig. 6). Based on the metabolic reconstruction of the obtained genome, we propose the name *Candidatus 'Methanoperedens nitroreducens'* and *Candidatus 'Methanoperedenaceae'* fam. nov. for the ANME-2d lineage (Supplementary Fig. 7).

A complete reverse methanogenesis pathway including all *mcr* subunit genes (*mcrABCDG*) and F420-dependent 5, 10-methylnetetrahydromethanopterin reductase (*mer*) genes were identified in the '*M. nitroreducens*' genome (Fig. 2). To our knowledge, this is the first report of a full reverse methanogenesis pathway in an ANME organism. The presence of a complete reductive acetyl-CoA (carbon fixation) pathway and acetyl-CoA synthetase (Fig. 2) suggest that '*M. nitroreducens*' may be able to produce acetate, as predicted for ANME-1 (refs 8, 9). We also identified genes for nitrate reduction but not subsequent steps in denitrification. The membrane-bound

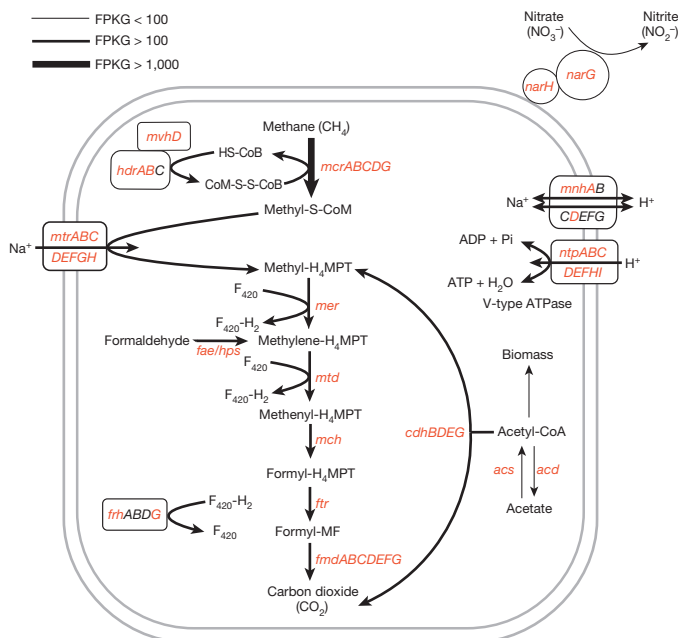


**Figure 2 | Key carbon and nitrogen transformations in '*Methanoperedens nitroreducens*'.** Reverse methanogenesis pathway in '*M. nitroreducens*' coupled by an unknown electron carrier to nitrate reduction. Highly expressed genes are shown in red, indicating that the complete reverse methanogenesis pathway and nitrate reduction genes were active in the bioreactor. Increasing line thickness indicates increasing absolute gene-expression values. FPKG (fragments mapped per kilobase of gene length) is a measure of normalized gene expression.

observed. The concentration of nitrite was negligible throughout the experiment. **b**, Fluorescence *in situ* hybridization micrograph of the bioreactor community showing the dominant '*M. nitroreducens*' population in large, dense clusters (green), smaller flanking *Kuenenia* cells (magenta) and other bacteria (blue).

nitrate reductase is comprised of a molybdopterin oxidoreductase domain and twin-arginine signal peptide for translocation across the membrane (*narG*) and iron-sulphur centres (*narH*). The *narGH* genes seem to have been acquired laterally from a bacterial donor (Supplementary Figs 6, 8 and 9). To confirm that the inferred lateral transfer was not the result of a chimaeric archaeal-bacterial assembly, we validated the metagenomic scaffolds using mate-pair and paired-end read information (Supplementary Figs 5 and 10). Furthermore, we sequenced a single '*M. nitroreducens*' cell isolated and identified previously using 16S rRNA analysis<sup>16</sup>, and mapped individual and assembled single-cell reads to the near-complete '*M. nitroreducens*' population genome, confirming the fidelity of the original assembly, including the region of putative lateral gene transfer (Supplementary Table 6 and Supplementary Fig. 6). The '*M. nitroreducens*' *narGH* originated from the Proteobacteria (Supplementary Figs 8 and 9), adding further weight to previous reports that the *nar* complex can be transferred laterally between phylogenetic domains<sup>17</sup>. Codon usage profiles show that the introduced genes have adapted to their archaeal host (Supplementary Table 7 and Supplementary Fig. 11), suggesting that the identified lateral transfer occurred well before the establishment of the population in the bioreactor.

Metatranscriptomics and isotope labelling experiments were carried out on the bioreactor and subsamples of the biomass, respectively, to confirm the expected expression of metabolic pathways and fate of methane and nitrate in the system. All genes necessary for oxidation of methane to carbon dioxide were highly expressed relative to housekeeping genes in '*M. nitroreducens*' (Fig. 2 and Supplementary Table 4), consistent with process data (Fig. 1a). No other genes or transcripts for anaerobic or aerobic methane oxidation<sup>18</sup> were detected in the metagenome or metatranscriptome. Further experiments confirmed that methane fed to the batch reactor was converted to carbon dioxide (Supplementary Fig. 12) and the added <sup>13</sup>C-labelled methane was converted to <sup>13</sup>C-labelled carbon dioxide (Fig. 3a). The MCR-specific inhibitor, 2-bromoethanesulphonate (BES), has been shown to inhibit AOM at low concentration (1 mM)<sup>19</sup>. However, BES inhibition tests using high concentrations (20 and 50 mM) did not have measurable effects on the AOM rates (Supplementary Fig. 13). The inability of BES to inhibit AOM in ANME is consistent with previous reports<sup>20,21</sup> and is potentially explained by impermeability of the ANME cell wall as has previously been proposed for cultured methanogens<sup>22</sup>.

Concomitant with the high expression of genes responsible for reverse methanogenesis in the bioreactor, the *narGH* genes belonging to '*M. nitroreducens*' were also highly expressed relative to housekeeping genes. A small number of *narGH* homologues identified in the metagenome belonging to flanking populations were not highly expressed indicating that '*M. nitroreducens*' performed the great majority of nitrate reduction in the bioreactor (Fig. 1a, Supplementary Table

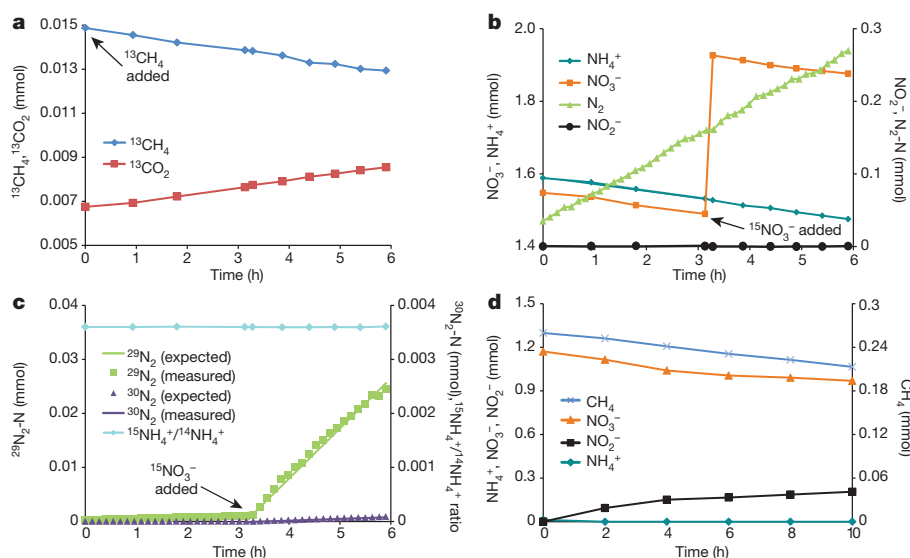


**Figure 3 | Methane oxidation coupled to nitrate reduction in the AOM bioreactor.** **a, b,** Data from isotope labelling batch test demonstrating stoichiometrically balanced conversion of  $^{13}\text{CH}_4$  to  $^{13}\text{CO}_2$  (**a**), and  $\text{NO}_3^-$  and  $\text{NH}_4^+$  to  $\text{N}_2$  without accumulation of  $\text{NO}_2^-$  (**b**). **c,** Experimentally measured production of  $^{29}\text{N}_2$  and  $^{30}\text{N}_2$  matching predictions (green and purple lines, respectively) based on assumed reactions (see details in Methods). The ratios between  $^{15}\text{NH}_4^+$  and  $^{14}\text{NH}_4^+$  are shown to confirm that there was no

8). To determine whether the *Kuenenia* anammox population uses the nitrite produced by '*M. nitroreducens*', a subsample of the bioreactor was fed unlabelled nitrate and ammonium (Fig. 3b) before addition of  $^{15}\text{N}$ -labelled nitrate (Fig. 3c). In this scenario, we expected accumulation of  $^{29}\text{N}$ -labelled dinitrogen gas as a result of anaerobic oxidation of  $^{14}\text{NH}_4^+$  with  $^{15}\text{NO}_2^-$ . Mass spectrometry results confirmed the production of  $^{29}\text{N}$ -labelled dinitrogen gas, according to reaction stoichiometry (Fig. 3c). The key genes for anaerobic ammonium oxidation by

conversion of  $^{15}\text{NO}_3^-$  to  $^{15}\text{NH}_4^+$ .  $^{30}\text{N}$ -labelled dinitrogen gas also increased as predicted, albeit to a much smaller extent, owing to reaction between  $^{15}\text{NO}_2^-$  and naturally present  $^{15}\text{NH}_4^+$ . The ratios between  $^{15}\text{NO}_3^-$  and  $^{14}\text{NO}_3^-$  in the system before and after  $^{15}\text{NO}_3^-$  addition were stable (data not shown). **d,** Batch test showing the accumulation of nitrite as a result of nitrate reduction when ammonium was removed from the feed.

the flanking *Kuenenia* population were highly expressed relative to their housekeeping genes (Supplementary Table 9). In further tests without ammonium feeding, we observed accumulation of nitrite in a subsample of the bioreactor (Fig. 3d), reconfirming the role of anammox in nitrite removal. Taken together, these data provide compelling evidence that '*M. nitroreducens*' couples AOM to nitrate reduction to nitrite, (equation (1)<sup>23</sup>).



$$(\Delta G^\circ = -503 \text{ kJ mol}^{-1} \text{ CH}_4)$$

The original rationale for operating the bioreactor with ammonium was based on the hypothesis that anammox bacteria would out-compete '*Methylomirabilis oxyfera*' for nitrite according to known reaction rates<sup>24</sup>, thus removing the main competitor to '*M. nitroreducens*' for methane and simplifying the analysis of AOM (Fig. 4a). Multiple lines of evidence (isotope labelling, electron and mass balance calculations, and metatranscriptomic data) confirm this hypothesis and indicate that in the presence of ammonium, nitrite produced by '*M. nitroreducens*' is used as an electron acceptor for ammonium oxidation to dinitrogen gas by the flanking *Kuenenia* population

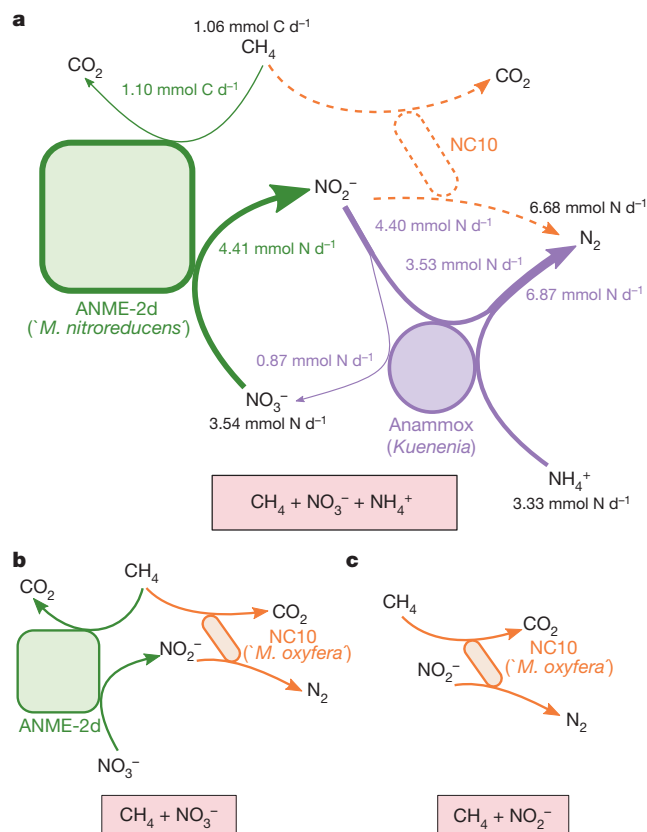


**Figure 4 | Observed interactions between key populations in methane-fed bioreactors with differing nitrogen sources.** Each population and its associated metabolic activities are colour-coded. **a,** Interactions under methane, nitrate and ammonium conditions in the current study. The thicknesses of arrows indicate reaction flux rates, and dashed arrows represent interactions not occurring under the given conditions (see Supplementary Table 10 for mass balance calculations). The methane consumption ( $1.10 \text{ mmol C d}^{-1}$ ) and dinitrogen gas production ( $6.87 \text{ mmol N d}^{-1}$ ) rates predicted based on measured ammonium, nitrate and nitrite data closely match their measured rates ( $1.06 \text{ mmol C d}^{-1}$  and  $6.68 \text{ mmol N d}^{-1}$ ) with only 3.8% and 2.8% errors, respectively. Mass and electron balance and molecular data further indicate that all of the methane consumed was used for reduction of nitrate to nitrite by '*M. nitroreducens*', and all of the produced nitrite ( $4.41 \text{ mmol N d}^{-1}$ ) was consumed by *Kuenenia* ( $4.40 \text{ mmol N d}^{-1}$ ). The outcompeted NC10 population is shown in dashed lines with no shading. **b,** Interactions in a bioreactor fed with methane and nitrate resulting in a co-culture of ANME-2d and '*M. oxyfera*'. **c,** Interactions in a bioreactor fed with methane and nitrite resulting in a dominant '*M. oxyfera*' population<sup>3,14</sup>.



(Figs 1a and 4a, Supplementary Table 9 and Supplementary Table 10). This partnership is also beneficial for '*M. nitroreducens*' as *Kuenenia* partially replenishes the nitrate (Fig. 4a). Consistent with this partnership, we found spatial co-localization of '*M. nitroreducens*' and the *Kuenenia* population (Fig. 1b and Supplementary Fig. 14). In the absence of ammonium, '*M. oxyfera*' would not have to compete with *Kuenenia* leading to the previously reported co-culture of a ANME-2d species and '*M. oxyfera*' (Fig. 4b). With nitrite as the only electron acceptor, '*M. nitroreducens*' is unable to compete with '*M. oxyfera*' (Fig. 4c), leading to a community dominated by the latter organism<sup>14</sup>. The significance of these different experimental scenarios in natural environments remains to be determined. However, our data conclusively demonstrate that '*M. nitroreducens*' is capable of coupling nitrate reduction to AOM as evidenced by closed electron and mass balance calculations and sole attribution of this metabolic activity to '*M. nitroreducens*' in the simplified bioreactor community.

## METHODS SUMMARY

A 5.6 litre bioreactor fed with nitrate, ammonium and methane was inoculated with a microbial consortium performing nitrate-dependent AOM and another performing anammox. Bioreactor operation was carried out as described previously<sup>14</sup>. For batch tests, subsamples of the bioreactor biomass were transferred to 330-ml vessels, which were provided with methane, nitrate and in most cases ammonium. In isotopic batch tests, <sup>13</sup>C-labelled methane and <sup>15</sup>N-labelled nitrate were added. <sup>13</sup>CH<sub>4</sub> and <sup>13</sup>CO<sub>2</sub> were measured with gas chromatography-mass spectrometry and isotope ratio mass spectrometry. <sup>15</sup>NO<sub>3</sub><sup>-</sup> and <sup>15</sup>NH<sub>4</sub><sup>+</sup> were measured with a continuous flow elemental analyser-isotope ratio mass spectrometer<sup>25</sup>. <sup>28</sup>N<sub>2</sub>, <sup>29</sup>N<sub>2</sub> and <sup>30</sup>N<sub>2</sub> were measured with a membrane inlet mass spectrometer<sup>3</sup>.

Bioreactor microbial community composition was determined using 16S rRNA gene amplicon pyrosequencing<sup>26</sup> and fluorescence *in situ* hybridization<sup>27</sup>. Metagenomic data was generated from a paired-end library sequenced on an Illumina HiSeq2000. The '*M. nitroreducens*' genome was binned using guanine-cytosine content, average contig coverage, and an emergent self-organizing map based on contig tetranucleotide frequencies<sup>28</sup>. The binned contigs were scaffolded using a 3-kb-insert mate-pair library sequenced on an Ion Torrent Personal Genome Machine. Annotation of the genome was performed using the Integrated Microbial Genomes Expert Review system<sup>29</sup> and curated manually. To validate laterally transferred regions in the '*M. nitroreducens*' genome, single cells were sorted, whole-genome amplified<sup>16</sup> and sequenced on Illumina GAII. Individual and assembled reads from the single cell were mapped against the '*M. nitroreducens*' genome and coverage values were determined. For metatranscriptomics, total RNA was extracted, ribosomal RNA subtracted, and complementary DNA synthesized (as described previously<sup>30</sup> with modifications) before sequencing on an Illumina MiSeq. Reads were mapped against the metagenome and gene expression was determined by calculating the number of fragments mapped per kilobase of gene length (FPKG). Highly expressed genes were identified by comparing FPKG values to those of housekeeping genes (Supplementary Table 4).

**Full Methods** and any associated references are available in the online version of the paper.

Received 2 October 2012; accepted 11 June 2013.

Published online 28 July 2013.

1. Beal, E. J., House, C. H. & Orphan, V. J. Manganese- and Iron-Dependent Marine Methane Oxidation. *Science* **325**, 184–187 (2009).
2. Boetius, A. *et al.* A marine microbial consortium apparently mediating anaerobic oxidation of methane. *Nature* **407**, 623–626 (2000).
3. Ettwig, K. F. *et al.* Nitrite-driven anaerobic methane oxidation by oxygenic bacteria. *Nature* **464**, 543–548 (2010).
4. Raghoebarsing, A. A. *et al.* A microbial consortium couples anaerobic methane oxidation to denitrification. *Nature* **440**, 918–921 (2006).
5. Hu, S. *et al.* Enrichment of denitrifying anaerobic methane oxidizing microorganisms. *Environmental Microbiol. Rep.* **1**, 377–384 (2009).
6. Knittel, K. & Boetius, A. Anaerobic oxidation of methane: progress with an unknown process. *Annu. Rev. Microbiol.* **63**, 311–334 (2009).
7. Reeburgh, W. S. Oceanic Methane Biogeochemistry. *Chem. Rev.* **107**, 486–513 (2007).
8. Hallam, S. J., Girguis, P. R., Preston, C. M., Richardson, P. M. & DeLong, E. F. Identification of methyl coenzyme M reductase A (*mcrA*) genes associated with methane-oxidizing archaea. *Appl. Environ. Microbiol.* **69**, 5483–5491 (2003).
9. Meyerdieters, A. *et al.* Metagenome and mRNA expression analyses of anaerobic methanotrophic archaea of the ANME-1 group. *Environ. Microbiol.* **12**, 422–439 (2010).

10. Stokke, R., Roalkvam, I., Lanzen, A., Hafflidason, H. & Steen, I. H. Integrated metagenomic and metaproteomic analyses of an ANME-1-dominated community in marine cold seep sediments. *Environ. Microbiol.* **14**, 1333–1346 (2012).
11. Heller, C., Hoppert, M. & Reiter, J. Immunological localization of coenzyme M reductase in anaerobic methane-oxidizing archaea of ANME 1 and ANME 2 type. *Geomicrobiol. J.* **25**, 149–156 (2008).
12. Scheller, S., Goenrich, M., Boecher, R., Thauer, R. K. & Jaun, B. The key nickel enzyme of methanogenesis catalyses the anaerobic oxidation of methane. *Nature* **465**, 606–608 (2010).
13. Milucka, J. *et al.* Zero-valent sulphur is a key intermediate in marine methane oxidation. *Nature* **491**, 541–546 (2012).
14. Hu, S., Zeng, R. J., Keller, J., Lant, P. A. & Yuan, Z. Effect of nitrate and nitrite on the selection of microorganisms in the denitrifying anaerobic methane oxidation process. *Environmental Microbiol. Rep.* **3**, 315–319 (2011).
15. Strous, M. *et al.* Deciphering the evolution and metabolism of an anammox bacterium from a community genome. *Nature* **440**, 790–794 (2006).
16. Yilmaz, S., Haroon, M. F., Rabkin, B. A., Tyson, G. W. & Hugenholtz, P. Fixation-free fluorescence *in situ* hybridization for targeted enrichment of microbial populations. *ISME J.* **4**, 1352–1356 (2010).
17. Cabello, P., Roldán, M. D. & Moreno-Vivián, C. Nitrate reduction and the nitrogen cycle in archaea. *Microbiology* **150**, 3527–3546 (2004).
18. Trotsenko, Y. A. & Murrell, J. C. in *Advances in Applied Microbiology* Vol. 63 (eds Sariaslani, S., Laskin, A. I. & Geoffrey, M. G.) 183–229 (Academic Press, 2008).
19. Nauhaus, K., Treude, T., Boetius, A. & Krüger, M. Environmental regulation of the anaerobic oxidation of methane: a comparison of ANME-I and ANME-II communities. *Environ. Microbiol.* **7**, 98–106 (2005).
20. Orcutt, B., Samarkin, V., Boetius, A. & Joye, S. On the relationship between methane production and oxidation by anaerobic methanotrophic communities from cold seeps of the Gulf of Mexico. *Environ. Microbiol.* **10**, 1108–1117 (2008).
21. Dekas, A. E., Poretsky, R. S. & Orphan, V. J. Deep-sea archaea fix and share nitrogen in methane-consuming microbial consortia. *Science* **326**, 422–426 (2009).
22. Smith, M. R. Reversal of 2-bromoethanesulfonate inhibition of methanogenesis in *Methanosarcina* sp. *J. Bacteriol.* **156**, 516–523 (1983).
23. Caldwell, S. L. *et al.* Anaerobic oxidation of methane: mechanisms, bioenergetics, and the ecology of associated microorganisms. *Environ. Sci. Technol.* **42**, 6791–6799 (2008).
24. Luesken, F. A. *et al.* Simultaneous nitrite-dependent anaerobic methane and ammonium oxidation processes. *Appl. Environ. Microbiol.* **77**, 6802–6807 (2011).
25. Brooks, P. D., Stark, J. M., McInteer, B. B. & Preston, T. Diffusion method to prepare soil extracts for automated nitrogen-15 analysis. *Soil Sci. Soc. Am. J.* **53**, 1707–1711 (1989).
26. Kunin, V., Engelbrektson, A., Ochman, H. & Hugenholtz, P. Wrinkles in the rare biosphere: pyrosequencing errors can lead to artificial inflation of diversity estimates. *Environ. Microbiol.* **12**, 118–123 (2010).
27. Glöckner, F. O. *et al.* An *in situ* hybridization protocol for detection and identification of planktonic bacteria. *System. Applied Microbiol.* **19**, 403–406 (1996).
28. Dick, G. J. *et al.* Community-wide analysis of microbial genome sequence signatures. *Genome Biol.* **10**, R85 (2009).
29. Markowitz, V. M. *et al.* IMG ER: a system for microbial genome annotation expert review and curation. *Bioinformatics* **25**, 2271–2278 (2009).
30. Stewart, F. J., Ottesen, E. A. & DeLong, E. F. Development and quantitative analyses of a universal rRNA-subtraction protocol for microbial metatranscriptomics. *ISME J.* **4**, 896–907 (2010).

**Supplementary Information** is available in the online version of the paper.

**Acknowledgements** We thank the ACE sequencing team; M. Butler, F. May and S. Low for their help with the 454 pyrosequencing, Illumina and Ion Torrent sequencing and the DOE Joint Genome Institute for single-cell sequencing. We also thank P. Lu for assistance with bioreactor operation, R. Zeng and P. Lant for their contribution to the development of initial bioreactors, B. Keller, J. Li, Y. Rui and Y. Wang for chemical and isotopic analyses, and D. Willner for assistance with genomic analysis. We are grateful to J. Euzéby for etymological advice. This work is supported by the Australian Research Council (ARC) through projects DP0666762 and DP0987204 and strategic funds from the Australian Centre for Ecogenomics. G.W.T. is supported by an ARC Queen Elizabeth II Fellowship (DP1093175). P.H. is supported by an ARC Discovery Outstanding Researcher Award (DP120103498). Y.S. is supported by the China Scholarship Council.

**Author Contributions** S.H. and Y.S. enriched the microorganisms in the parent bioreactor and performed batch and isotope labelling tests. S.H., Y.S., J.K. and Z.Y. performed the process data analysis. M.F.H. performed the sampling, preservation and nucleic acid extractions. M.F.H. prepared samples for single-cell genomics, metagenomic and metatranscriptomic sequencing. M.F.H. and G.W.T. performed the microbial community analysis. M.I. developed the bioinformatic tools. M.F.H., M.I., P.H. and G.W.T. performed the bioinformatic analyses. M.F.H., S.H., Z.Y., P.H., G.W.T. wrote the manuscript in consultation with all other authors.

**Author Information** Sequencing data are deposited at the NCBI Short Read Archive under accession numbers SRR925398, SRR925402 and SRR901892. Annotated assembled sequences were incorporated into the IMG system with the Taxon Object ID 2515154041. Reprints and permissions information is available at [www.nature.com/reprints](http://www.nature.com/reprints). The authors declare no competing financial interests. Readers are welcome to comment on the online version of the paper. Correspondence and requests for materials should be addressed to G.W.T. ([g.tyson@uq.edu.au](mailto:g.tyson@uq.edu.au)) or Z.Y. ([z.yuan@awmc.uq.edu.au](mailto:z.yuan@awmc.uq.edu.au)).

## METHODS

**Bioreactor operation, nutrient and gas measurements.** The bioreactor was inoculated from two previously established bioreactors, one performing nitrate-dependent AOM<sup>5</sup> and the other performing anammox with a nitrite, ammonium and methane feed. Using group-specific FISH probes (see FISH section below), the AOM inoculum was dominated by ANME-2d (60%) and '*M. oxyfera*' (30%), and the anammox bioreactor was dominated by *Kuenenia*-like planctomycetes (50%) and '*M. oxyfera*' (20%). At the time of sampling, the nitrate consumption rate of the AOM bioreactor was approximately  $1.1 \text{ mmol l}^{-1} \text{ d}^{-1}$ , the volatile suspended solids (VSS) concentration was approximately  $0.8 \text{ g l}^{-1}$ , the nitrite loading rate for the anammox bioreactor was approximately  $1.4 \text{ mmol l}^{-1} \text{ d}^{-1}$ , and the VSS concentration was approximately  $1.1 \text{ g l}^{-1}$ . Equal volumes of the two inocula (500 ml) were mixed with 3.6 l of medium<sup>4</sup> in a 5.6 l glass bioreactor.

The bioreactor was operated at room temperature ( $22 \pm 2^\circ \text{C}$ ) and mixed continuously with a magnetic stirrer at 200 r.p.m. To provide methane as the carbon and energy source, a mixed gas (5%  $\text{N}_2$ , 90%  $\text{CH}_4$  and 5%  $\text{CO}_2$ ) was used to flush the headspace regularly to maintain the methane partial pressure between 0.5 and 1.0 atm. The pH of the bioreactor was monitored with a pH probe (TPS) and controlled between 7.0 and 7.5 by manual injection of a 1 M HCl solution. Other operational conditions are as described previously<sup>14</sup>. The concentration of nitrate and ammonium in the bioreactor was maintained between 5.0 and  $10.0 \text{ mmol l}^{-1}$  by manual injection of concentrated stock solutions ( $80 \text{ g NO}_3^- \text{--} \text{N l}^{-1}$  and  $48 \text{ g NH}_4^+ \text{--} \text{N l}^{-1}$ , respectively). Stock solutions were prepared with degassed milli-Q water and stored in sealed bottles with nitrogen in the headspace.

**Fluorescence in situ hybridization.** Cells from the bioreactor were collected and fixed in 4% paraformaldehyde before FISH<sup>27</sup>. Bioreactor microbial communities were hybridized with the following oligonucleotide probes; ANME-2-specific probe (Darch872-FITC)<sup>4</sup>, anammox-specific probe (AMX820-Cy3)<sup>31</sup>, '*M. oxyfera*'-specific probe (DBACT193-Cy3)<sup>4</sup> and a general bacterial probe (EUB338+-Cy5)<sup>32</sup> (final concentration of 5 ng for each probe) for 2 h at  $46^\circ \text{C}$ . Labelled cells were visualized on an LSM512 confocal laser scanning microscope (Carl Zeiss) with Ar-ion laser (488 nm) and two HeNe lasers (543 and 633 nm). To determine the spatial arrangement of '*M. nitroreducens*' and anammox cells, 15 images were acquired at random locations in each well. All images were processed using the DAIME software<sup>33</sup> and split into individual colour channels before image segmentation. Cells were identified using the automatic segmentation in the DAIME and artefacts (irregular shapes and bright autofluorescence) were rejected manually. Segmentation was performed for all images using the 'batch processing' option. Spatial co-localization analysis was performed using the Linear Dipole algorithm in DAIME.

**DNA extraction.** DNA was extracted from 2 ml of bioreactor biomass using a FastDNA SPIN Kit for Soil (MP Biomedicals) with Fastprep beadbeater (Bio101) according to manufacturer's instructions. DNA concentrations were quantified using the Quant-iT dsDNA HS assay kit (Invitrogen) as per the manufacturer's instructions.

**Microbial community profiling.** 16S rRNA genes were amplified using the 'universal' primer set 926F/1392R<sup>26</sup>. PCR products were purified using a QIAquick PCR Purification Kit (Qiagen) and quantified using Quant-iT dsDNA HS assay kit (Invitrogen). Amplicons were pooled in equimolar concentrations and sequenced using a 454 GS FLX Titanium sequencer (Roche) as per the manufacturer's protocol.

Amplicon sequences were processed using the ACE Pyrotag Pipeline (APP) v.2.3.2 (<http://github.com/ECogenomics/APP>). In brief, sequences were quality filtered and de-multiplexed with the split\_libraries.py script of QIIME v.1.3.0 using default parameters<sup>34</sup> and then checked for chimaeras against Greengenes database<sup>35</sup> using UCHIME<sup>36</sup>. Sequences less than 350 bp in length were removed. Homopolymeric errors were corrected using Acacia v.1.48 (ref. 37). Sequences with 97% identity were clustered as operational taxonomic units (OTUs) using UCLUST<sup>38</sup> and then taxonomically assigned using the Greengenes database.

**Metagenomic sequencing and assembly.** Community genomic DNA from the bioreactor was sheared to approximately 500 bp using a Covaris-S2 instrument (Covaris) and a paired-end library was prepared using the TruSeq PE Cluster Kit v3-cBot-HS and TruSeq SBS kit v3-HS sequencing kit (Illumina). The library was sequenced on the HiSeq 2000 (Illumina) platform generating  $2 \times 150$ -bp paired-end reads with an average insert length of 250 bp.

Reads were filtered based on quality score and reads less than 100 bp in length were removed using CLC Genomic Workbench v.5.1.5 (CLC bio). Filtered sequences were assembled using CLC's *de novo* assembler using a *k*-mer length of 63. The average coverage of each contig > 1 kb was quantified by mapping all the reads using CLC Genomics Workbench with a minimum 95% similarity and 95% of the read length.

To separate the '*M. nitroreducens*' genome from other organisms in the metagenome, we used a combination of read coverage, guanine-cytosine content

and tetranucleotide frequencies<sup>28</sup> calculated using *kmer\_counter* ([http://github.com/wwood/bioruby-kmer\\_counter](http://github.com/wwood/bioruby-kmer_counter)). Redundancy analysis was performed on these data and visualized as a principal component analysis plot using the R packages *vegan* and *ggplot2* respectively (<http://www.r-project.org/>). The metagenome was also binned using an emergent self-organizing map (ESOM; <http://www.cbs.dtu.dk/courses/27618.chemo/ESOM.pdf>) as described previously<sup>28</sup>. In brief, tetranucleotide frequencies were clustered on a toroidal map with Euclidean grid distance and dimensions scaled to  $160 \times 268$ . Training used the K-Batch algorithm ( $k = 0.15\%$ ) for 20 training epochs. The standard best match search method was used with local best match radius of 8. Contig fragments with similar tetranucleotide patterns were clustered and different genome bins were manually identified as areas separated by distinct ridge lines.

To scaffold the binned '*M. nitroreducens*' contigs, a 3-kb-insert mate-paired library was prepared according to the Ion Mate-Paired Library protocol (Life Technologies) and subsequently sequenced using a Ion 316 chip on an Ion Torrent Personal Genome Machine (PGM) (Life Technologies). Forward and reverse mate-pairs were extracted and mapped against the binned contigs. Scaffolds were constructed based on the mate-pair links between the contigs using *ionPairer* (<http://github.com/ECogenomics/ionPairer>). To check the completeness and fidelity of the assembly, an essential single-copy gene analysis was performed using AMPHORA2 (ref. 39). The near-complete '*M. nitroreducens*' genome was submitted to IMG/ER<sup>29</sup> for gene calling and functional annotation. Coding sequences were assigned a unique identifier prefixed with 'ANME2D'. Annotations for the methane and nitrogen genes were confirmed manually. Codon usage profiles were calculated using *CodonW* (<http://codonw.sourceforge.net/>).

**Single-cell genomic sequencing and assembly validation.** A single amplified '*M. nitroreducens*' cell generated as part of a previous study<sup>16</sup> was sequenced (75-bp PE reads) using an Illumina Genome Analyser II. Reads were mapped onto the '*M. nitroreducens*' genome and the bioreactor metagenomic contigs using *bwa* v.0.6.2-r126 (ref. 40) with default settings. *Samtools* v0.0.18 (ref. 41) was used to calculate the percentage of mapped reads. The '*M. nitroreducens*' scaffolds were cut into a total of 3,205 non-overlapping 1-kb windows and the log median coverage was calculated for each window using the '*M. nitroreducens*'-only mapping and a custom Perl script.

**Phylogenetic inference.** For protein-coding genes, homologues were identified in reference genomes available through IMG, and imported into ARB<sup>42</sup>. Amino acid sequences were aligned using *ClustalW*, and phylogenies were calculated using parsimony and maximum likelihood (*PhyIip*, *PROTPARS*). For 16S rRNA gene phylogenetic analysis, sequences were aligned using *NAST*<sup>43</sup>, and imported into ARB. Phylogenetic trees were constructed by using neighbour joining and maximum-likelihood methods.

For the genome tree, all finished and draft bacterial and archaeal genomes were downloaded from the IMG4.0 (<http://img.jgi.doe.gov/>). Hidden Markov models (HMMs) for a set of 38 essential single-copy genes were obtained from the authors of *PhyloSift* (<http://phylosift.wordpress.com/>; Supplementary Table 4). Candidate single-copy conserved genes from the IMG genomes were identified and aligned to the HMMs using *HMMER3* (ref. 44). Unaligned characters were masked out and the resulting sequences were concatenated. A phylogenetic tree with estimated branch support values was constructed from these concatenated alignments using *FastTree* v.2.1.3 (ref. 45) with default settings and visualized in ARB.

**Metatranscriptomics.** A subsample of the bioreactor biomass (approximately 10 ml) was collected and RNA was extracted using RNA PowerSoil Total RNA Isolation kit (MO-BIO) according to manufacturer's protocol. Turbo DNA-free kit (Ambion) was used to remove genomic DNA and purified using RNeasy MinElute cleanup kit (Qiagen). rRNA subtraction was performed using Ribo-Zero Magnetic kit (Epicentre) as per the manufacturer's instructions. rRNA subtracted total RNA was amplified using *MessageAmp II Bacteria* kit (Ambion) as described previously<sup>46</sup>. Amplified RNA was reverse transcribed to cDNA using the *SuperScript III First-Strand Synthesis System* (Invitrogen) via random hexamer primers and *SuperScript Double-Stranded cDNA synthesis kit* (Invitrogen) as described previously<sup>30</sup> before sequencing library preparation. Libraries were prepared using an Illumina *Nextera DNA sample preparation kit* according to the manufacturer's instructions, with the following modifications. During the PCR cleanup with *Agencourt AMPure XP magnetic beads* (Beckman Coulter Genomics), the ratio of beads to sample was increased to 1.8:1 to capture smaller fragments. The library was then sequenced on the Illumina *MiSeq* (150 base pair paired end reads).

Sequences were mapped against the metagenome using *BWA* v.0.6.2 (ref. 40). For quantification of gene expression, the number of reads that mapped against a particular gene was normalized by the length of the gene to generate a number of fragments mapped per kilobase of gene length (FPKG) using the *sam2fpgk.pl* script v.0.1 (<http://github.com/minilinin/sam2fpgk>), which was subsequently

used to determine their expression relative to housekeeping genes (Supplementary Table 4).

**Batch experiments.** Isotopic labelling experiments were conducted in triplicate in 330-ml stirred glass vessels without headspace, enabling methane consumption to be easily determined. A subsample of bioreactor biomass (380 ml) was transferred to each vessel, with the excess 50 ml of biomass stored in a reservoir bottle connected to the lid of the vessel through a tube. The biomass was flushed with a mixed gas (90% CH<sub>4</sub>, 5% CO<sub>2</sub>, 5% N<sub>2</sub>) for 30 min. Sixty millilitres of <sup>13</sup>C-labelled methane gas (Sigma Aldrich, 99 atom % <sup>13</sup>C) was injected through the septum, displacing the equivalent amount of biomass into the reservoir bottle. After 30 min, the gaseous <sup>13</sup>C-labelled methane was removed from the system by displacement with the biomass from the reservoir bottle. Nitrate and ammonium were added to the vessel by injecting concentrated anaerobic stock solutions to reach a concentration between 3.6–7.1 mmol N l<sup>-1</sup>. Three hours after the experiments started, <sup>15</sup>N-labelled nitrate was injected to achieve a concentration of 1.4 mmol <sup>15</sup>NO<sub>3</sub><sup>-</sup> l<sup>-1</sup>, which was approximately 20–30% of the total nitrate present. The experiment was then continued for 3 h. The headspace of the reservoir bottle was flushed with helium continuously during the experiment to keep it oxygen-free. Liquid samples were collected from the sampling port at the middle of the vessel and filtered using 0.22-µm filters and stored in vacuum tubes (BD Vacutainer). To compensate for liquid losses due to sampling, the valve between the vessel and the reservoir was opened during sampling, and the dilution effect of the extra biomass/liquid brought into the vessel was taken into account during data processing.

Isotopically labelled samples containing nitrate and ammonium were processed with a method described previously<sup>25</sup> and the isotopic fractions were measured by EA-IRMS with a Eurovector Elemental Analyzer (Isoprime-EuroEA 3000). The dissolved methane and carbon dioxide concentrations and their isotopic fractions were measured with GC-MS-IRMS. <sup>28</sup>N<sub>2</sub>, <sup>29</sup>N<sub>2</sub> and <sup>30</sup>N<sub>2</sub> were measured in real-time using membrane inlet mass spectrometer (MIMS)<sup>3</sup>, the sum of which gave the total N<sub>2</sub> concentration. The measured <sup>28</sup>N<sub>2</sub>, <sup>29</sup>N<sub>2</sub> and <sup>30</sup>N<sub>2</sub> were compared with their predicted values based on the assumption that nitrate was reduced to nitrite by '*M. nitroreducens*' and all the produced nitrite was removed by *Kuenenia* through the anammox reaction. The production rates of <sup>29</sup>N<sub>2</sub> and <sup>30</sup>N<sub>2</sub> dinitrogen gas after <sup>15</sup>N-labelled nitrate addition were predicted as:

$$r^{29}\text{N}_2\text{-N} = {}^{15}\text{N}\% \text{ of } \text{NO}_3^- \times {}^{14}\text{N}\% \text{ of } \text{NH}_4^+ \times r\text{NH}_4^+ + {}^{14}\text{N}\% \text{ of } \text{NO}_3^- \times {}^{15}\text{N}\% \text{ of } \text{NH}_4^+ \times r\text{NH}_4^+$$

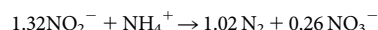
$$r^{30}\text{N}_2\text{-N} = {}^{15}\text{N}\% \text{ of } \text{NO}_3^- \times {}^{15}\text{N}\% \text{ of } \text{NH}_4^+ \times r\text{NH}_4^+$$

Batch experiments were also conducted in triplicate to observe the nitrogen conversion in the absence of ammonium. For each test, a subsample of bioreactor biomass was transferred to a stirred glass vessel (330 ml) after ammonium in the bioreactor was depleted. The biomass was flushed with the mixed gas (described above) for 30 min to saturate with methane. Nitrate was then added to reach a concentration of approximately 3.6 mmol l<sup>-1</sup>. Each test was run for approximately 10 h. Liquid samples were taken every 2 h for the analysis of dissolved methane, ammonium, nitrite and nitrate concentrations as described previously<sup>14</sup>.

For BES inhibition tests, 260 ml of bioreactor biomass was added per 330 ml batch vessel, with methane, ammonium and nitrate added as described above. BES was added to two sets of triplicate vessels 24 h after initiation of the experiment to a final concentration of 20 mM and 50 mM, respectively. Methane, dinitrogen gas, ammonium, nitrite and nitrate concentrations were monitored with the method described previously<sup>14</sup>.

**Mass and electron balance calculations.** The consumption rate of methane (rCH<sub>4</sub>), ammonium (rNH<sub>4</sub><sup>+</sup>), nitrate (rNO<sub>3</sub><sup>-</sup>) and nitrite (rNO<sub>2</sub><sup>-</sup>), and production rate of dinitrogen gas (rN<sub>2</sub>-N) were determined from the respective measured

concentration profiles through linear regression (see Supplementary Table 10). Nitrogen balance was calculated as the difference between the measured dinitrogen gas production rate and the sum of the measured ammonium and nitrate consumption rates: rN<sub>2</sub>-N - (rNH<sub>4</sub><sup>+</sup> + rNO<sub>3</sub><sup>-</sup>). The percentage error was calculated as the ratio between nitrogen balance error and the measured dinitrogen gas production rate: (rN<sub>2</sub>-N - (rNH<sub>4</sub><sup>+</sup> + rNO<sub>3</sub><sup>-</sup>))/rN<sub>2</sub>-N. Electron balance was calculated as the difference between the electrons required by the reduction of nitrate to dinitrogen gas and the electrons produced by the oxidation of ammonium to dinitrogen gas and methane to CO<sub>2</sub>: -5 × rNO<sub>3</sub><sup>-</sup> + 3 × rNH<sub>4</sub><sup>+</sup> + 8 × rCH<sub>4</sub>. The percentage error was calculated as the ratio between electron balance error and electrons required by the reduction of nitrate to dinitrogen gas: (-5 × rNO<sub>3</sub><sup>-</sup> + 3 × rNH<sub>4</sub><sup>+</sup> + 8 × rCH<sub>4</sub>)/-5 × rNO<sub>3</sub><sup>-</sup>. The nitrite consumption rate and nitrate production rate of anammox were calculated based on the ammonium consumption rate (rNH<sub>4</sub><sup>+</sup>) and anammox reaction stoichiometry<sup>47</sup>:



The net nitrate reduction rate was calculated as the sum of measured nitrate consumption rate (rNO<sub>3</sub><sup>-</sup>) and nitrate production rate of anammox reaction. The methane consumption rate was predicted based on the net nitrate reduction rate and equation (1), and compared with measured methane consumption rate (rCH<sub>4</sub>). The dinitrogen gas production rate was predicted as the sum of the measured ammonium and nitrate consumption rates (rNH<sub>4</sub><sup>+</sup> + rNO<sub>3</sub><sup>-</sup>), and compared with the measured dinitrogen gas production rate (rN<sub>2</sub>-N).

- Schmid, M., Schmitz-Esser, S., Jetten, M. & Wagner, M. 16S-23S rDNA intergenic spacer and 23S rDNA of anaerobic ammonium-oxidizing bacteria: implications for phylogeny and in situ detection. *Environ. Microbiol.* **3**, 450–459 (2001).
- Daims, H., Brühl, A., Amann, R., Schleifer, K.-H. & Wagner, M. The domain-specific probe EUB338 is insufficient for the detection of all bacteria: development and evaluation of a more comprehensive probe set. *Systematic Applied Microbiol.* **22**, 434–444 (1999).
- Daims, H., Lückner, S. & Wagner, M. Daime, a novel image analysis program for microbial ecology and biofilm research. *Environ. Microbiol.* **8**, 200–213 (2006).
- Caporaso, J. G. et al. QIIME allows analysis of high-throughput community sequencing data. *Nature Meth.* **7**, 335–336 (2010).
- McDonald, D. et al. An improved Greengenes taxonomy with explicit ranks for ecological and evolutionary analyses of bacteria and archaea. *ISME J.* **6**, 610–618 (2012).
- Edgar, R. C., Haas, B. J., Clemente, J. C., Quince, C. & Knight, R. UCHIME improves sensitivity and speed of chimera detection. *Bioinformatics* **27**, 2194–2200 (2011).
- Bragg, L., Stone, G., Imelfort, M., Hugenholtz, P. & Tyson, G. W. Fast, accurate error-correction of amplicon pyrosequences using Acacia. *Nature Meth.* **9**, 425–426 (2012).
- Edgar, R. C. Search and clustering orders of magnitude faster than BLAST. *Bioinformatics* **26**, 2460–2461 (2010).
- Wu, M. & Scott, A. J. Phylogenomic analysis of bacterial and archaeal sequences with AMPHORA2. *Bioinformatics* **28**, 1033–1034 (2012).
- Li, H. & Durbin, R. Fast and accurate short read alignment with Burrows–Wheeler transform. *Bioinformatics* **25**, 1754–1760 (2009).
- Li, H. et al. The Sequence Alignment/Map format and SAMtools. *Bioinformatics* **25**, 2078–2079 (2009).
- Ludwig, W. et al. ARB: a software environment for sequence data. *Nucleic Acids Res.* **32**, 1363–1371 (2004).
- DeSantis, T. Z. et al. NAST: a multiple sequence alignment server for comparative analysis of 16S rRNA genes. *Nucleic Acids Res.* **34**, W394–W399 (2006).
- Eddy, S. R. Accelerated profile HMM searches. *PLOS Comput. Biol.* **7**, e1002195 (2011).
- Price, M. N., Dehal, P. S. & Arkin, A. P. FastTree 2—approximately maximum-likelihood trees for large alignments. *PLoS ONE* **5**, e9490 (2010).
- Shi, Y., Tyson, G. W. & DeLong, E. F. Metatranscriptomics reveals unique microbial small RNAs in the ocean's water column. *Nature* **459**, 266–269 (2009).
- Kuenen, J. G. Anammox bacteria: from discovery to application. *Nature Rev. Microbiol.* **6**, 320–326 (2008).

## ERRATUM

doi:10.1038/nature12619

### **Erratum: Anaerobic oxidation of methane coupled to nitrate reduction in a novel archaeal lineage**

Mohamed F. Haroon, Shihu Hu, Ying Shi, Michael Imelfort, Jurg Keller, Philip Hugenholtz, Zhiguo Yuan & Gene W. Tyson

*Nature* **500**, 567–570 (2013); doi:10.1038/nature12375

In this Letter, equation (1) was inadvertently shown incorrectly, with CO<sub>2</sub> missing from the reaction products. The correct equation (1) is shown below:



This has been corrected in the HTML and PDF versions of the original manuscript.